ELSEVIER

Physica B 271 (1999) 1–6

PHYSICA B

www.elsevier.com/locate/physb

Excitonic effect in resonant Raman scattering by 2LO-phonon in CdS and ZnSe

Prabhat Verma[a,*], S. Anand[b], K.P. Jain[b]

[a]*Institute of Theoretical Physics, Freiberg University of Mining and Technology, B.-v.-Cotta-Str. 4, 09596 Freiberg, Germany*
[b]*Department of Physics, Indian Institute of Technology, New Delhi 110 016, India*

Received 15 February 1999; received in revised form 1 June 1999; accepted 17 August 1999

Abstract

Two-LO-phonon resonant Raman scattering has been performed on pure and doped CdS and ZnSe samples and the results are analyzed in terms of excitonic theory assuming correlated electron–hole pairs as intermediate states in the transition process. Good agreement with experimental results is found. The excitons involved in the intermediate transitions are short lived for the doped samples compared to the pure sample. The resonance profile for the doped samples can be better explained by considering the involvement of excitons with larger magnitudes of $\boldsymbol{k}$.

PACS: 78.30.Fs; 63.20.Kr; 71.35.Gg

Keywords: Resonant Raman scattering; Excitons; Phonons; CdS; ZnSe

1. Introduction

Raman scattering from wide band-gap material provides important information on the critical physical properties of a crystal [1]. For resonant Raman scattering (RRS), electronic structure plays an important role in Raman process [2] since the photon energy lies in the vicinity of the band gap of the semiconductor. The intermediate virtual electronic transition becomes real and its strength is only limited by the finite lifetime broadening of the electronic states involved in the excitation process. In contrast to many other optical techniques, RRS provides information about both the lattice dynamics and the electronic structure of the semiconductor at the same time. Furthermore, RRS not only allows one to study the electron–phonon interaction, but also to differentiate between the Fröhlich and the deformation potential interaction using symmetry considerations. In direct band-gap materials, first-order Raman scattering corresponds to optical phonons restricted to the center of the Brillouin zone with the condition $\boldsymbol{q} \approx 0$. In second-order RRS, on the other hand, phonons can have wave vectors $\boldsymbol{q}_1$ and $\boldsymbol{q}_2$ all over the Brillouin zone as long as they are nearly equal in magnitude and have opposite directions. Therefore, RRS by two phonons contains more information about the electron–phonon interaction and the $\boldsymbol{q}$ dependence of the same can be studied.

* Present address: Department of Electronics and Information Science, Kyoto Institute of Technology, Matsugasaki, Sakyo-ku, Kyoto 606, Japan. Tel.: +81-75-724-7439; Fax: +81-75-724-7400.

E-mail address: verma@dj.kit.ac.jp (P. Verma)

0921-4526/99/$ - see front matter
PII: S0921-4526(99)00241-0

Over the past years, RRS by one- and two-phonons has been the subject of many investigations in several III–V and II–VI binary and ternary compound semiconductors [3–9]. The nature of the intermediate states involved in the scattering process has remained a subject of discussion. Several models based on the uncorrelated electron–hole pairs or the free-electron theory (FET) were developed for RRS process [10,11], but they were criticized because they were in disagreement with experimental observations. One reason for the failure of the FET models is that they show only outgoing resonance, and, second is that they require a lifetime broadening which is much smaller than the broadening observed in other optical experiments, suggesting that the assumption of uncorrelated electron–hole pairs as intermediate states in the transition process is not suitable. The failure of uncorrelated electron–hole pair theory to explain the experimental observations led to the necessity of including electron–hole correlation. Now the role of excitons in one-phonon RRS process is well studied [4,8,12,13] and it is understood that Wannier excitons are the intermediate states in one-phonon RRS process. However, two-phonon RRS was mostly treated with FET and there has been only limited [14,15] work on the two-phonon resonance where involvement of excitons was considered.

The aim of this paper is to interpret the experimental results of 2LO-phonon RRS from pure and doped CdS and ZnSe samples using the excitonic model. Good agreement obtained between experimental and theoretical resonance profiles indicates that the intermediate states in the transition process for 2LO-phonon are correlated electron–hole pairs. It is observed that the excitonic widths are increased due to the presence of impurity atoms in doped samples. The experimental RRS profile for 2LO-phonon in doped samples shows better agreement with the calculated profile when intermediate excitons in the transition process are considered with larger magnitudes of $\boldsymbol{k}$.

2. Experimental details

Samples used for the present study are pure CdS, lithium-doped CdS, lithium-doped ZnSe and iodine-doped ZnSe bulk materials, which will be denoted by CdS, CdS : Li, ZnSe : Li and ZnSe : I, respectively. Apart from ZnSe : I, all samples were grown from the melt, and, where applicable, impurities were introduced by diffusion. ZnSe : I crystal was grown by the chemical vapor transport (CVT) method using iodine as the transporting agent. The details of growth process and the basic optical properties of this sample are discussed elsewhere [16,17]. Raman scattering experiments were performed using Jobin Yvon or Spex monochromator, CCD or PMT detectors and usual optics and electronics. All samples were investigated at low temperature with the visible lines of an Ar-ion laser. A tunable cw dye laser operating with stilbene 3 and pumped by the ultraviolet lines of the Ar-ion laser was also used for CdS samples. For ZnSe samples, resonance profiles were obtained by a combination of wavelength tuning (where probing energy is varied at a fixed sample temperature) and band-gap tuning (where sample temperature is varied at a fixed probing energy) methods. In the latter method, the resonance condition is achieved by changing the band gap of the material. However, the results can be converted into a form which is of the type of the form used for the former method by assuming the band gap to be fixed and then calculating an equivalent change in the probing energy.

3. Review of theory

In order to explain our experimental results, we will use the theoretical model discussed by García-Cristóbal et al. [14], which was successfully used by the authors to interpret their experimental results on some of the III–V semiconductors. It is therefore useful to present a review of this theoretical model in the form which will be used to interpret experimental results of the present work. In Ref. [14], a rigorous calculation is presented for 2LO-phonon Raman scattering efficiency (RSE) for a direct band-gap material. The scattering process was treated with perturbation theory in the framework of the effective mass approximation by considering Wannier excitons (correlated electron-hole pairs) as intermediate electronic states and the Fröhlich interaction between excitons and phonons. It is

usual to express the measured Raman intensities in terms of RSE, $ds/d\Omega$, which is related to the scattering amplitude, W_{FI}, by [2]

$$\frac{ds}{d\Omega}(\omega) = \frac{V}{(2\pi)^2}\frac{\omega\eta\omega_s^3\eta_s^3}{c^4}\frac{1}{(\hbar\omega)^2}\sum_F |W_{FI}|^2, \quad (1)$$

where ω (ω_s) and η (η_s) are frequency and refractive index of the incident (scattered) light, V is the crystal volume, and c is the velocity of light. The scattering amplitude W_{FI} is the transition probability from the initial state I to the final state F of the scattering process, which can be given as [14]

$$W_{FI} = \sum_{\alpha,\beta,\gamma} \frac{C}{(\hbar\omega - E_\alpha + i\Gamma_\alpha)(\hbar\omega - \hbar\omega_0 - E_\beta + i\Gamma_\beta)(\hbar\omega - 2\hbar\omega_0 - E_\gamma + i\Gamma_\gamma)}, \quad (2)$$

where α is the initial state of the intermediate exciton, β and γ are the excitonic states after emission of the first and the second phonons, respectively, E and Γ are the energies and the widths of the corresponding excitonic states, $\hbar\omega_0$ is the energy of one-LO-phonon, and C can be treated as a normalization constant, which includes the matrix elements for the exciton–radiation and the exciton–lattice interaction Hamiltonians. The samples studied in the present work have three valence bands corresponding to the $j_z = \pm\frac{3}{2}$ holes, the $j_z = \pm\frac{1}{2}$ holes and the split-off holes, and therefore three different excitonic branches are expected to participate in the scattering process. For wurtzite CdS, however, the average mass of heavy and light holes is the same, therefore, heavy and light holes need not be considered separately. In the resonant conditions near the fundamental gap, contribution from heavy holes is much larger than the other two, so that only one contribution to the scattering amplitude may be considered for ZnSe samples as well. However, we found that it was necessary to include the contribution from light holes for doped ZnSe samples.

The intermediate states discussed in Ref. [14] include the discrete (d) and the continuum (c) states of the excitonic spectra. RSE has several contributions depending upon the sequence of intermediate states (e.g., $c \to c \to c$, $d \to d \to d$, $c \to d \to c$, etc.), where each transition contributes to the scattering amplitude, and hence, RSE includes a sum of scattering amplitudes over all transition sequences. The final expression for 2LO-phonon RSE can be written as [14]

$$\frac{ds}{d\Omega}(\omega) = S\left(\frac{\hbar\omega + 2\hbar\omega_0}{\hbar\omega}\right)^2 \int_0^\infty dQ \frac{1}{Q^2}|\sum W_{FI}(Q)|^2, \quad (3)$$

where the summation runs over different contributions among discrete and continuous states, and the integrand is dimensionless with $Q = qa$, $\boldsymbol{q}$ being phonon wave vector and a the exciton Bohr radius. The constant term S includes the exciton binding energy, the Fröhlich coupling constant and the interband matrix element. It is shown in Ref. [14] that the most important contributions to the RSE comes from the sequences $c \to d \to d$, $d \to d \to d$ and $c \to c \to d$. We therefore consider only these sequences under the summation in Eq. (3). The detailed expressions for various contributions in W_{FI} were obtained from Ref. [14], and Eq. (3) was first solved analytically and then RSE was calculated numerically to obtain fits to the experimental results.

4. Results and discussion

The absolute value of RSE in experiment is obtained from the raw data by using a sample substitution method with the LO-phonon line of a Si sample as a reference [18]. The measured scattering rate R in the raw data and the absorption coefficient α of the semiconductor are related to Raman efficiency by [2,8]

$$\frac{ds}{d\Omega}(\omega) = \frac{\alpha^*(\omega)}{\alpha(\omega)}\frac{R(\omega)}{R^*(\omega)}\frac{ds^*}{d\Omega}(\omega), \quad (4)$$

where quantities with the asterisk refer to Si. The absolute values of RSE for Si are obtained from the empirical relation [8]

$$\frac{ds^*}{d\Omega}(\omega) = (7.75\times10^{-5})(\hbar\omega - 3.4)^{-4}, \quad (5)$$

with $\hbar\omega$ in eV. Eq. (4) was used to calculate the experimental absolute value of RSE for all samples. In the present work, we do not calculate the theoretical absolute value of RSE and focus attention only on the shape of the RSE profile. Therefore, in order to have a comparison, both theoretical expression and experimental values of RSE are normalized to one.

Fig. 1 shows the values of 2LO-phonon RSE for a pure CdS bulk sample measured in the $z(x,x)\bar{z}$ back scattering configuration from the $\langle 1\,0\,0\rangle$ surface, where the electron–phonon Fröhlich interaction is selected by the symmetry. Experimental data, which are presented by full circles in Fig. 1, show both incoming and outgoing resonance at energies $E_{1s} = E_g - R$ and $E_{1s} + 2\hbar\omega_0$, respectively, the latter being an order of magnitude stronger than the former, where E_g is the band-gap energy and R is the exciton binding energy. The theoretical fit calculated from Eq. (3) is presented by the solid line in Fig. 1. The excitonic widths were obtained from the experimental profile and the other parameters used in the calculation were obtained from various references listed in Table 1. Good agreement between experimental values and the theoretical fit is obtained, which indicates that 2LO-phonon RSE profile for this sample can be understood by invoking the excitonic model.

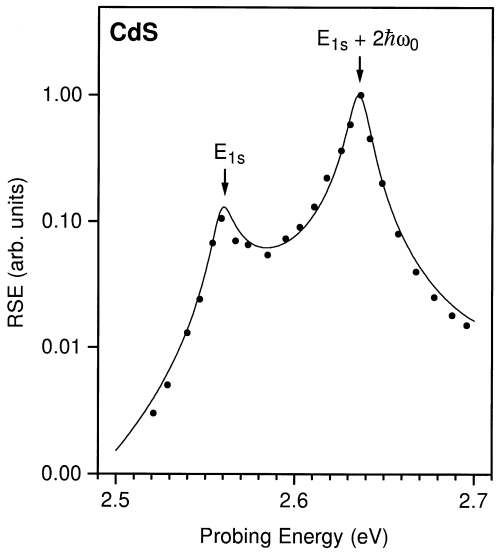

Fig. 1. Normalized RSE for 2LO-phonon in RRS from pure CdS sample measured at 4 K. Full circles present the experimental values and the curve presents a fit using Eq. (3) and parameters listed in Table 1. Vertical arrows indicate the position of the incoming and the outgoing resonance at energies $E_g - R$ and $E_g - R + 2\hbar\omega_0$, respectively.

Experimental data for 2LO-phonon RSE for CdS : Li are presented in Fig. 2. Experiments were performed under the same conditions as in the case of pure CdS. It can be observed that the positions of the incoming and the outgoing resonance are not affected by the presence of lithium impurities. We attempted to fit the experimental data with the same parameters which were used for pure CdS, and found that the experimental profile shows larger widths than the calculated ones. The theoretical curve agrees well with the experimental profile when we consider larger widths for the discrete exciton states. This can be explained in terms of an increased number of decay channels for an exciton in a discrete state due to the presence of impurity states. However, as this sample is only lightly doped, the band-gap energy is nearly unchanged. The solid line presented in Fig. 2 is calculated from Eq. (3) along with the parameters listed in Table 1.

ZnSe samples contain comparatively larger amount of impurity atoms. In earlier studies performed on these samples using Raman scattering, absorption spectroscopy and photoluminescence experiments, it was observed that the band edges of

Table 1
Numerical values of the parameters used for various samples for theoretical fits in Figs. 1–4. The band-gap energies for CdS samples are at 4 K and that for ZnSe samples are the effective band gaps at room temperature, which include shifts due to the presence of impurity atoms

Parameter	CdS	CdS : Li	ZnSe : Li	ZnSe : I
E_g (eV)	2.589[a]	2.589[a]	2.560[b]	2.556[b]
$\hbar\omega_0$ (meV)	38.0[c]	38.0[c]	31.4[b]	31.3[b]
R (meV)	30.2[a]	30.2[a]	19[a]	19[a]
m_e/m_h	0.3[a]	0.3[a]	0.19[a]	0.19[a]
Γ_d (meV)	4.0[d]	4.8[d]	7.0[d]	8.0[d]
Γ_c (meV)	15[d]	15[d]	19[d]	21[d]

[a] Ref. [19].
[b] Refs. [16,17].
[c] Ref. [20].
[d] From the fit to experimental values in the present work.

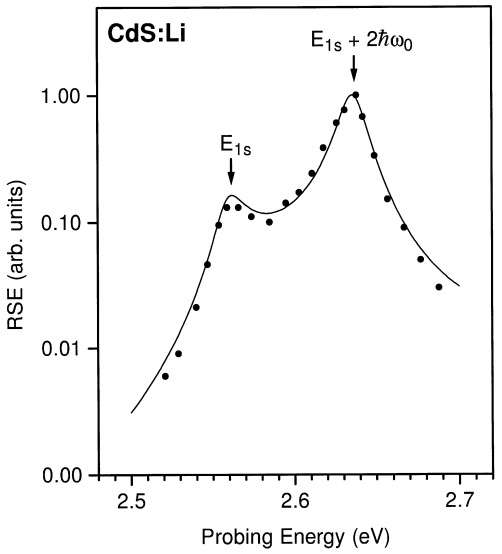

Fig. 2. Normalized RSE for 2LO-phonon in RRS from CdS : Li measured at 4K. Full circles present experimental values and the curve presents a fit using Eq. (3) and parameters listed in Table 1. The positions of the incoming and the outgoing resonance remain unchanged by the presence of impurity atoms.

these samples are shifted towards low energy due to the presence of large amount of impurity [16,17]. The observed band edges for ZnSe : Li and ZnSe : I at room temperature were found at 2.560 and 2.556 eV, respectively. Raman scattering experiments on these samples were performed in a normal back-scattering geometry, where both the Fröhlich and the deformation potential interaction could contribute to the electron–phonon interaction. However, as shown later, we could obtain reasonably good theoretical fits for these samples using Eq. (3), which indicates that the Fröhlich interaction remains the dominating process in the vicinity of resonance. Since the samples contain larger amounts of impurity atoms and the experiments include temperatures which correspond to an energy of the order of exciton binding energy, it is expected in Eq. (2) that the excitonic widths Γ will have larger values and the energies E will involve the effective band gap of the sample. Further, we found that the experimental RSE profiles for doped ZnSe samples, which show nearly equal strengths for the incoming and the outgoing resonance, cannot be explained with Eq. (3) by considering excitons with small magnitude of $\boldsymbol{k}$. By considering $\boldsymbol{k}$ with values larger by an order of magnitude in the calculation of the scattering amplitude W_{FI} and by involving contributions from the light holes, we obtained reasonably good fits to our experimental results for ZnSe : Li and ZnSe : I samples. Resultant profiles are shown in Figs. 3 and 4 for ZnSe : Li and ZnSe : I, respectively, which show fairly good agreement with the experimental profiles. The values of exciton widths used for these samples are about 50% larger than those listed in literature for pure ZnSe. These values are obtained from the fit and are listed in Table 1. This observation indicates that the intermediate excitons in heavily doped samples involve larger magnitudes of $\boldsymbol{k}$, and are short lived due to the presence of impurity states close to the excitonic states.

5. Conclusion

Experimental results on 2LO-phonon RRS for pure and doped CdS and ZnSe samples have been

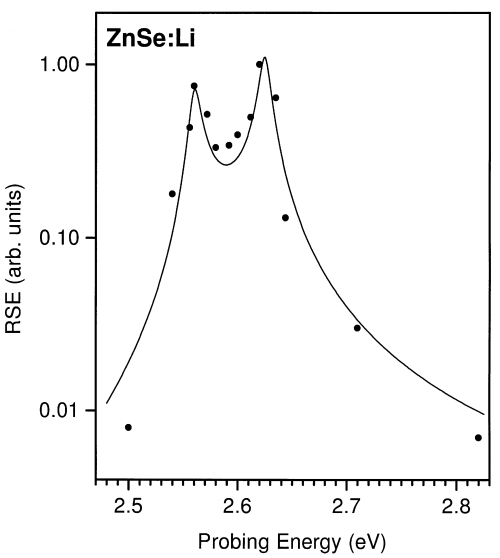

Fig. 3. Normalized RSE for 2LO-phonon in RRS from ZnSe : Li presented at room temperature. Full circles present experimental data and the curve presents a fit using Eq. (3) and parameters listed in Table 1.

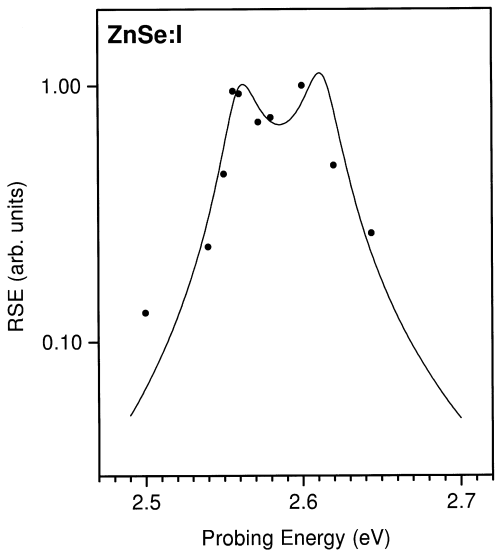

Fig. 4. Normalized RSE for 2LO-phonon in RRS from ZnSe:I presented at room temperature. Full circles present the experimental data and the curve presents a fit using Eq. (3) and parameters listed in Table 1.

analyzed using the excitonic model to explain the RSE profile, indicating that correlated electron–hole pairs are intermediate states in the scattering process for the samples discussed. Fröhlich interaction remains the dominant mechanism for the electron–phonon interaction near resonance even when the deformation potential interaction is also allowed by symmetry. Presence of impurity atoms in the doped samples provide additional decay channels for excitons and the excitonic widths are increased. It is found that the intermediate state excitons in the doped samples necessitate larger magnitudes of $\boldsymbol{k}$ than in pure or lightly doped samples. Good agreement between calculated and observed resonance profiles for heavily doped samples are obtained when larger magnitudes of $\boldsymbol{k}$ for the intermediate excitons are considered.

References

[1] M. Cardona (Ed.), Light Scattering in Solids, Topics in Applied Physics, Vol. 8, Springer, Berlin, 1975.
[2] M. Cardona, in: M. Cardona, G. Güntherodt (Eds.), Light Scattering in Solids II, Topics in Applied Physics, Vol. 50, Springer, Berlin, 1982, p. 19.
[3] K.P. Jain, C.S. Jayanthi, Phys. Rev. B 19 (1979) 4198.
[4] K.P. Jain, R.K. Soni, S.C. Abbi, Phys. Rev. B 31 (1985) 6820.
[5] R.K. Soni, Rita Gupta, K.P. Jain, Phys. Rev. B 33 (1986) 5560.
[6] W. Kauschke, M. Cardona, Phys. Rev. B 33 (1986) 5473.
[7] A.K. Sood, W. Kauschke, J. Menéndez, M. Cardona, Phys. Rev. B 35 (1987) 2886.
[8] W. Limmer, H. Leiderer, K. Jakob, W. Gebhardt, W. Kauschke, A. Cantarero, C. Trallero-Giner, Phys. Rev. B 42 (1990) 11325.
[9] H. Leiderer, W. Limmer, W. Gebhardt, J. Crystal Growth 101 (1990) 921.
[10] R. Zeyher, Phys. Rev. B 9 (1974) 4439.
[11] R.M. Martin, Phys. Rev. B 10 (1974) 2620.
[12] W. Kauschke, V. Vorlíček, M. Cardona, Phys. Rev. B 36 (1987) 9129.
[13] W. Limmer, H. Leiderer, K. Jakob, W. Gebhardt, in: E.M. Anastasakis, J.D. Joannopoulos (Eds.), Proceedings of the International Conference on the Physics of Semiconductors, World Scientific, Singapore, 1990, p. 2005.
[14] A. García-Cristóbal, A. Cantarero, C. Trallero-Giner, M. Cardona, Phys. Rev. B 49 (1994) 13430.
[15] A. García-Cristóbal, A. Cantarero, C. Trallero-Giner, W. Limmer, Phys. Stat. Sol. B 196 (1996) 443.
[16] S. Anand, P. Verma, S.C. Abbi, K.P. Jain, M.J. Tafreshi, K. Balakrishnan, R. Dhansekaran, Pramana, J. Phys. 47 (1996) 133.
[17] S. Anand, Ph.D. Thesis, University of Delhi, India, 1996 (unpublished).
[18] J. Wagner, M. Cardona, Solid State Commun. 48 (1983) 301.
[19] O. Madelung (Ed.), in: Semiconductors – Basic data Springer, Berlin:Germany 1996
[20] P. Verma, J. Kortus, J. Monecke, S. Anand, K.P. Jain, Phys. Rev. B 59 (1999) 15748.